Bull. Chem. Soc. Jpn., ***68***, *3423—3428(1995)*

Gelation of Fully Acylated Cellobiose in Alkane Solution

Nobuhiro Ide, Takeshi Fukuda,* and Takeaki Miyamoto

Institute for Chemical Research, Kyoto University, Uji, Kyoto 611

(Received July 13, 1995)

Cellobiose octa(decanoate), a discotic columnar mesogen, was found to form in hexadecane solution various molecular assemblies such as a lyotropic liquid crystal of discotic columnar type, multimolecular micelles, and a thermoreversible gel, depending on the concentration and temperature. The gelation, observed even at very low concentrations, say, <0.01 weight fraction of the mesogenic compound, is believed to proceed by local coagulation of long threadlike micelles into micro-liquid-crystallites, which work as cross-linking points combining the threadlike micelles. This will be a new type of gel that could be termed a "liquid crystalline gel."

The derivatization of carbohydrates has provided a vast source of thermotropic mesogens.$^{1-3)}$ Those derivatives with one or a few alkyl substituents have an amphiphilic character with hydrogen-bonding ability and form, in most cases, layered, columnar, or cubic phases.

Fully substituted inositols$^{4)}$ and cellooligosaccharides,$^{5-8)}$ which apparently lack the hydrogen-bonding ability, are also known to function as discotic columnar mesogens. Molecular shape or configuration as well as specific intermolecular interactions must play a key role in the structuring of these systems. For example, cellobiose octaalkanoate (CBn) is a flat molecule consisting of a rather hydrophilic cellobiose core surrounded by hydrophobic alkyl chains. Presumably because of this characteristic molecular structure, it forms, when the carbon number n of the acyl group is appropriate ($7\leq n\leq 14$), a thermotropic discotic columnar liquid crystal (LC), in which columns formed by a regular stacking of cellobiose moieties are packed into a two-dimensional hexagonal or rectangular lattice$^{5,6)}$ (Fig. 1). The fact that fully alkylated cellobiose shows no liquid crystallinity$^{9)}$ indicates that the carbonyl groups in the acyl derivatives also stabilize the columnar structure. It is also noted that CBn has two types of stereoisomers, i.e., the α- and β-anomers, with respect to the substituent configuration at the C1 carbon of the reducing end unit (cf. Fig. 1). It has been found that the α-anomer forms a more stable LC phase than the equivalent β-anomer.$^{10)}$

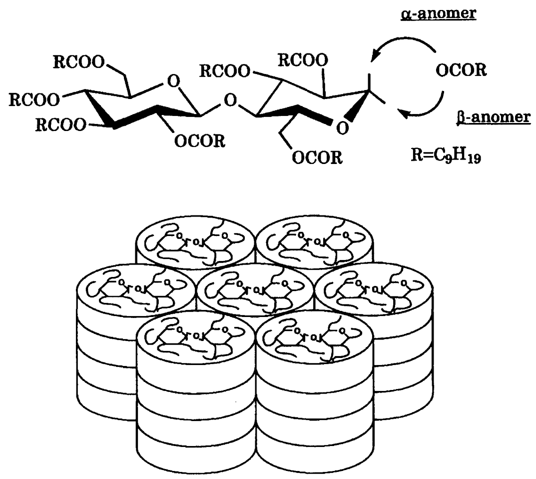

Fig. 1. Chemical structure of cellobiose octa(decanoate) and a schematic representation of its discotic columnar structuring.

While CBn is easily soluble and molecularly dispersed in common solvents like tetrahydrofuran and chloroform, it has been found to form, in selective-type solvents like alkanes, various molecular assemblies such as a lyotropic LC, multimolecular micelles, and a thermoreversible gel, depending on the concentration and temperature. This seems to be general, rather than exceptional, behavior of this type of mesogenic molecules in this type of solvents, and reminds us the function of certain amphiphilic compounds like 1,3 : 2,4-p,p'-ditolylidene sorbitol, which is known to be a powerful (nonmesogenic) agent to gel solutions by itself forming long threadlike micelles.$^{11)}$ This work is the first to report details of such behavior observed for cellobiose octa(decanoate) (CB10) dissolved in hexadecane (HD). The CB10 studied here is a nearly pure α-type compound.

Experimental

Sample Preparation. Commercially obtained decanoic acid and trifluoroacetic anhydride (TFAA) were used without further purification. β-Cellobiose (Nacalai Tesque, Japan) was vacuum dried before use. CB10 was synthesized by esterification of β-cellobiose according to the TFAA method$^{10)}$: a mixture of decanoic acid (100 g, 0.581 mol; 8 mol. amt. to hydroxyl groups of cellobiose) and TFAA (31 mL, 0.218 mol; 3 mol. amt. to the hydroxyl groups) was activated at 100 °C for 30 min, to which cellobiose (5 g; 1.47×10^{-2} mol) was added and the reaction was allowed to proceed at 100 °C for about 6 h. After it had cooled, the mixture was poured into a 20-fold excess of methanol. The precipitate was filtered off and further purified by reprecipitation with a chloroform (solvent)/methanol (nonsolvent) system several times. The entire absence of hydroxyl-related absorption in its infrared (IR) spectrum confirmed that the sample was a fully acylated derivative. The α/β anomeric ratio of CB10 was 97/3 by proton NMR.[10]

Tube-Inverting Test. The sol–gel transition temperature of the CB10/HD system was identified by the tube-inverting method. CB10 was mixed with HD in a sealed glass tube with a diameter of 8 mm, and the mixture was heated to about 100 °C to ensure a homogeneous solution. The solution was quenched to a predetermined temperature, kept at that temperature for a predetermined time, and then tested by inverting: The sealed sample tube was placed upside down in the water bath. If the solution flowed, it was defined as a sol, and if it did not, it was defined as a gel.

Thermal Analysis. Differential scanning calorimetry (DSC) was done on a Rigaku Denki DSC-8230, Japan, to obtain information on phase transitions. Before measurement, the sample in a sample pan was heated to about 120 °C to make a homogeneous solution. All measurements were made at a constant cooling rate of 10 °C min^{-1}.

Optical Microscopy. LC textures were observed by polarized optical microscopy (Optiphoto-Pol, Nikon, Japan) with a hot stage (FP-82 with central processor FP-80, Mettler, Switzerland).

X-Ray Diffraction. X-Ray diffraction patterns were recorded with a flat-plate camera using a Rigaku Denki X-ray generator Ru-3H, Japan, with graphite-filtered Cu $K\alpha$ radiation (1.542 Å). The film to specimen distance was measured by the calibration with silicon powder: A mixture of a sample solution and silicon powder sealed in a capillary with a diameter of 0.5 mm was heated to 120 °C to ensure homogeneous mixing, cooled down to the measurement temperature (50 °C or 55 °C), and kept at that temperature for 30 min before the measurement was started.

Infrared Measurement. A time-resolved infrared (IR) analysis was done with a JASCO FT/IR-8800, Japan, with a Mettler hot stage. The sample was placed between a stretched and folded Teflon® sheet in the hot stage.

Light Scattering. Dilute CB10 solutions were measured by static light scattering with a DLS-7000, Otsuka Electronics, Japan. The optical source was a He–Ne laser (wavelength $\lambda_0=632.8$ nm). The refractive index increment (dn/dc) was measured with a differential refractive spectrometer DRM1030, Otsuka Electronics, Japan.

Results and Discussion

Sol–Gel Diagram. The gelation time t_g, i.e., the time for the solution to gel after being quenched from a high temperature was found to depend on both concentration and temperature. Figure 2 shows the T vs. t_g plots for several values of w_1, where T is the temperature, and w_1 is the weight fraction of CB10. Each curve seems to level off at large values of t_g, which indicates that each solution has a critical temperature of gelation, T_g, above which the system never gels. Clearly t_g is a function of the "super cooling depth" $\Delta T = T_g - T$: when ΔT is large, the system gels very quickly, while gelation takes a long time when ΔT is small. We also note that the system with $w_1=0.85$ shows very small t_g even for small ΔT, and in this regard, it is different from other systems (with $w_1 \leq 0.8$). This implies that the structure of highly concentrated systems is different from that of the systems with a lower concentration ($w_1 \leq 0.8$). This in fact is the case, as will be shown later. The values of T_g approximately estimated with the data in Fig. 2 are plotted against w_1 in Fig. 3. As w_1 decreases from unity, T_g decreases sharply at first and then gradually for $w_1 \leq 0.8$.

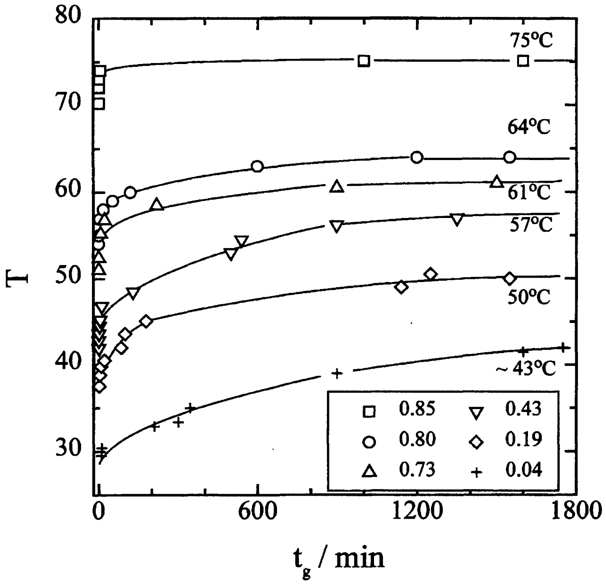

Fig. 2. Relations between temperature T and gelation time t_g for various values of w_1. The temperature figure attached to each curve is an approximate value of T_g.

Transition Temperatures by DSC. Figure 4 shows the DSC thermograms of CB10/HD mixtures. In the bulk, CB10, which is a nearly pure α-type anomer, forms a hexagonal ordered columnar phase, D_{ho}, in discotics at temperatures between the crystallization temperature $T_{c,1}$ of 47.4 °C and the isotropic–anisotropic transition temperature T_{ia} of 103.8 °C, and unlike its homologues with shorter acyl chains, it undergoes no mesomorphic transition.[10] As Fig. 4 shows, an exothermic peak assignable to the T_{ia} of the mixture system is detectable at concentrations down to about 0.87, while a peak corresponding to $T_{c,1}$ is observable for all examined mixtures. The crystallization temperature of HD, $T_{c,2}$, appears as the lowermost-temperature peak. These transition temperatures are also illustrated in Fig. 3. The T_{ia} temperatures observed for high-w_1 mixtures can be identified with the gelation temperatures T_g, which indicates that in this concentration regime, the system becomes immobilized by liquid crystalliza-

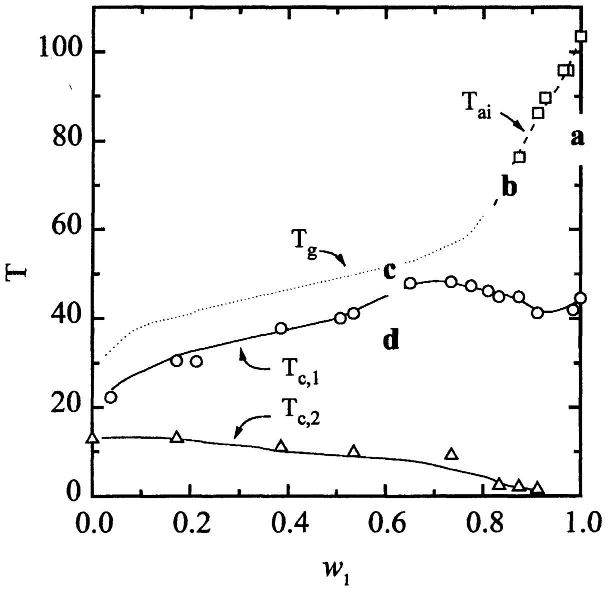

Fig. 3. Transition temperatures of the CB10/HD system.

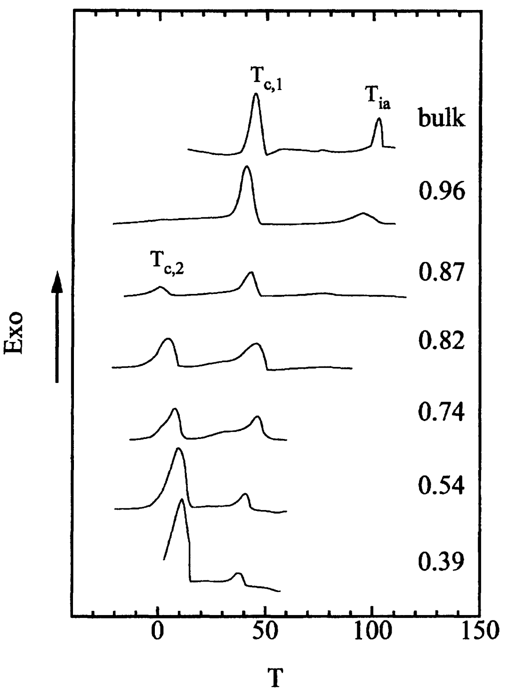

Fig. 4. DSC thermograms of CB10/HD mixtures.

tion rather than by gelation.

Optical Microscopic Textures. Polarized optical microscopic observations were made at points **a** through **d** indicated in Fig. 3, the micrographs being presented in Fig. 5. At point **a** is observed a fan-shaped texture characteristic of discotic columnar phases. A similar texture composed of smaller domains is observed at point **b**, which implies that system **b** is a homogeneous mesophase rather than a gel phase. System **c** is birefringent but shows no clear texture. It is very different from system **d**, which has a sharp-edged crystalline texture. This indicates that system **c** involves minute liquid crystalline phases.

X-Ray Diffraction. According to our previous work,[10] the X-ray diffractogram of oriented pure CB10 was characterized by three equatorial reflections with spacings (d_{100}, d_{110}, and d_{200}) being in the ratio $1:1/\sqrt{3}:1/2$ and one meridional reflection with a spacing (d_{001}) of 5.4 Å, which led to the mesophase structure in Fig. 1. In the (unoriented) mixture systems at 50 °C studied here, the 100 reflection ring could be observed at concentrations down to about 0.5, below which it was too weak to permit quantitative analysis. The 001 reflection ring could be detected at $w_1 \geq 0.8$, giving a constant d_{001} value of 5.4 Å independent of w_1. Although other reflections were generally too weak to give a definite answer, the above observations along with the photomicroscopic textures (Fig. 5) suggest that the mixture systems also form a discotic columnar phase with the axial periodicity (d_{001}) unchanged by the addition of HD.

Figure 6 shows the value of d_{100} as a function of w_1. As w_1 decreases from unity, d_{100} increases at first and becomes constant for $w_1 \leq 0.7$. This indicates that at $w_1 > 0.7$, the solvent HD "swells" the columnar structure only in the lateral direction. This would happen when HD is mixed with the alkyl moieties but does not get into the columnar cores of the cellobiose moieties. The dotted line in Fig. 6 was calculated by the relationship

$$d_{100}(w_1) = \left(1 + \frac{v_2}{v_1}\frac{1-w_1}{w_1}\right)^{\frac{1}{2}} d_{100}(1) \qquad (1)$$

which is based on the assumption that HD contributes only to the lateral expansion of the system. Here v_1 and v_2 are the specific volumes of CB10 and HD, respectively, and $d_{100}(1)$ is the value of d_{100} for the pure CB10. The experimental data for $w_1 \geq 0.7$ are well represented by this relation. The constancy of d_{100} for $w_1 \leq 0.7$ indicates that in this region the LC phase can accommodate no more HD and the system becomes biphasic with a HD-saturated LC phase and an isotropic phase with low w_1.

FT-IR Analysis. It was observed that the carbonyl absorption band of pure CB10 at around 1750 cm^{-1} significantly shifts before and after the mesomorphic transition. This is seen in Fig. 7a, which shows the temperature dependence of the mean wavenumber $\bar{\nu}$, defined as the wavenumber at the center-of-mass position of the carbonyl absorption band. The isotropic-anisotropic transition accompanies a sharp decrease of $\bar{\nu}$ of about 6 cm^{-1}, indicating that the columnar structuring is significantly stabilized by an energetic interaction, perhaps of dipole–dipole type, among the carbonyl groups.[12] Thus the carbonyl band can be used as a measure for the structuring of the system.

Figure 7b shows the time dependence of $\bar{\nu}$ for the system with $w_1 = 0.42$ at 59 °C. The solution was heated to 110 °C to ensure homogeneous mixing, quenched to 59 °C (a few degree above the gelation threshold; see

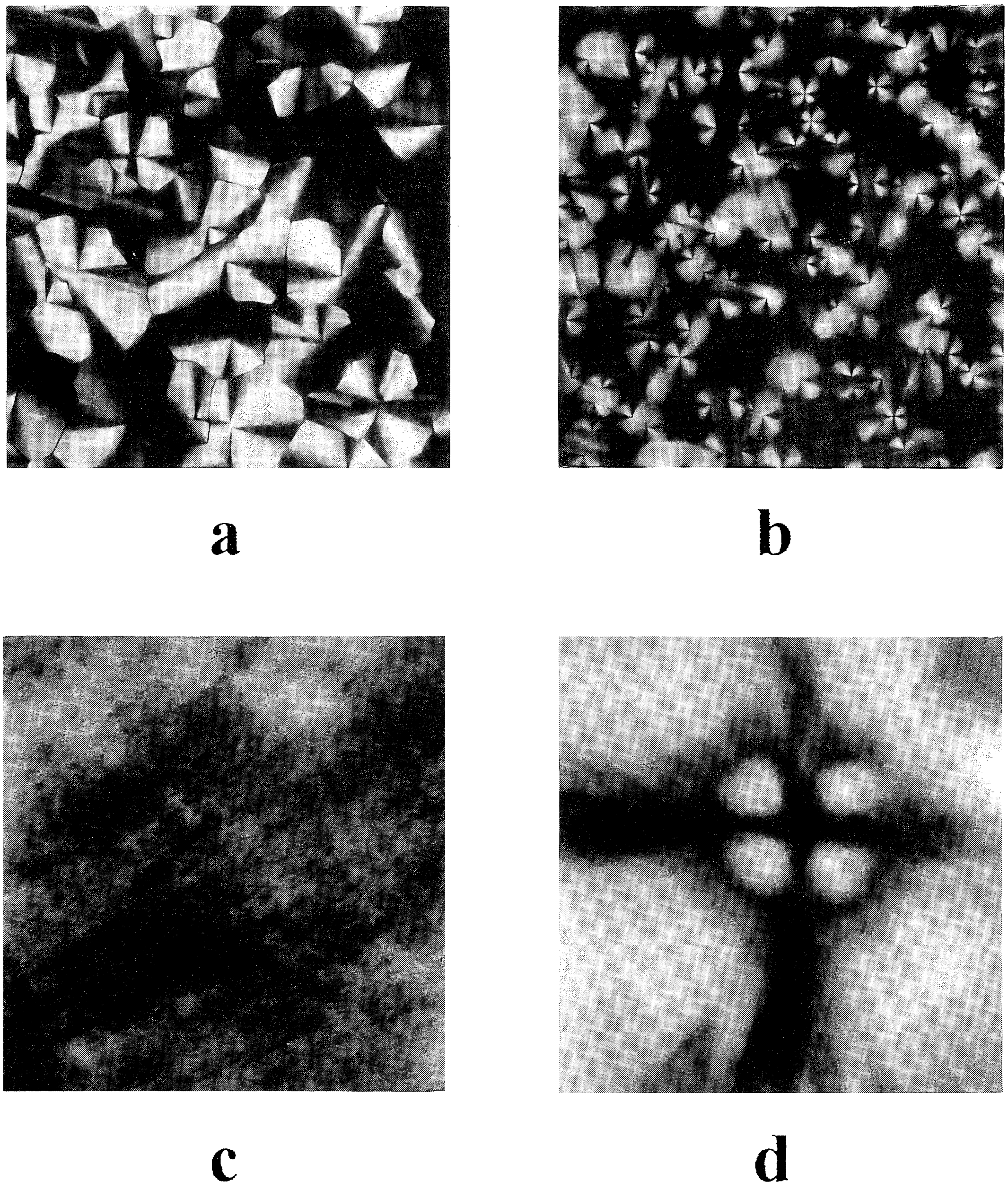

Fig. 5. Polarized optical micrographs of the CB10/HD mixtures observed at points **a** through **d** in Fig. 3.

Fig. 3), and IR analyzed. The $\overline{\nu}$ at time zero is close to the value shown by the bulk isotropic phase, while the $\overline{\nu}$ observed after a long time ($t\cong 10$ h) is similar to the value for the bulk LC phase. This strongly indicates that as time elapses, the molecules come together forming a special type of cluster, probably a rodlike or threadlike micelle, that causes the shift of the IR band.

Light Scattering. Figure 8 shows the plot of $(Kc/R_\theta)^{1/2}$ vs. $\sin^2(\theta/2)$ for a dilute solution ($c=3.45\times10^{-4}$ g mL^{-1}) of CB10 at 25 °C, just above the sol–gel transition temperature T_g of this solution. Here K is the optical constant, and R_θ is the reduced excess scattering intensity at scattering angle θ. The figure gives an apparent molecular weight of about 2.8×10^6 and an apparent root-mean-square radius of gyration of about 2300 Å. This radius is anomalously large for the molecular weight, and it suggests that the molecules are clustering into a highly asymmetric assembly: if we assume, for example, that CB10 molecules regularly stack face to face to form a rigid rodlike micelle of the observed molecular weight, we estimate its radius of gyration to be about 3000 Å, a value rather close to the one observed. This result is consistent with what was suggested by the IR analysis above.

Conclusion

Figure 9 illustrates the phase diagram and the state of molecular dispersion of the CB10/HD system deduced from these analyses. In region "LC" the system is of single phase—a discotic hexagonal columnar phase with the hexagonal lattice size increasing with the increasing HD fraction. The isotropization temperature T_i ($\cong T_\mathrm{ai}$)

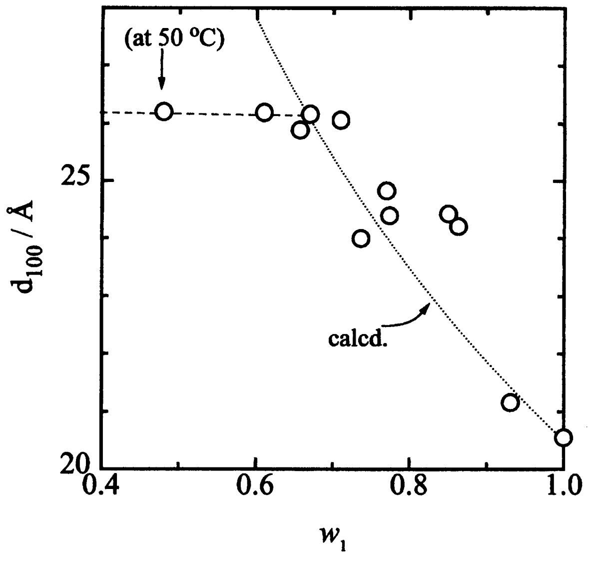

Fig. 6. The X-ray d_{100} spacing as a function of CB10 concentration w_1. The dotted line was calculated by Eq. 1 (see text).

decreases from 105 °C at $w_1=1.0$ to 60 °C at $w_1=0.75$. In the two regions "LC gel" and "C gel", the system shows the appearance of gel: The LC gel includes a liquid crystalline phase, while the C gel has a crystalline phase. The gelation in this system should have a close relevance to the discotic columnar phase formed in concentrated solutions and the bulk. Namely, it is presumed that there is a region, just above the critical gelation temperature, in which CB10 molecules stack face to face forming long threadlike micelles. The gelation proceeds below the critical temperature by local coagulation of the micelles into micro-liquid-crystallites (or micro-crystallites at lower temperatures), which work as cross-linking points that combine the long threadlike micelles (Fig. 10). This is a slow process requiring hours.

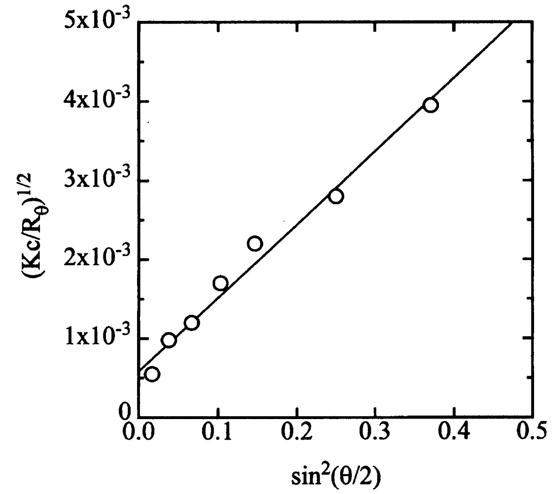

Fig. 8. Plot of $(Kc/R_\theta)^{1/2}$ vs. $\sin^2(\theta/2)$ for a dilute CB10/HD solution ($c=3.45\times10^{-4}$ g mL^{-1}, $T=25$ °C).

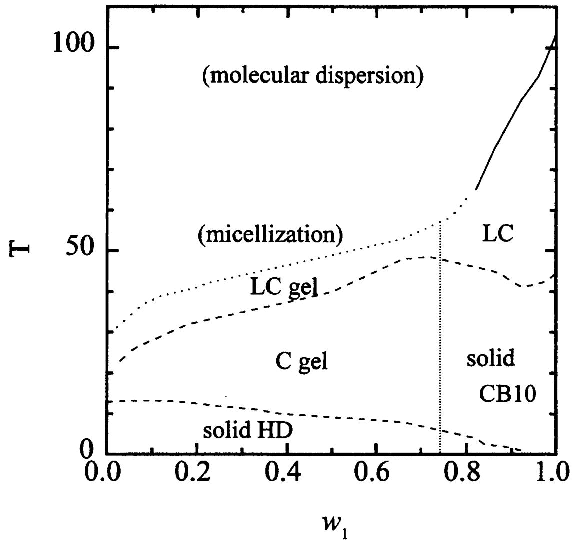

Fig. 9. Phase diagram of the CB10/HD system (see text).

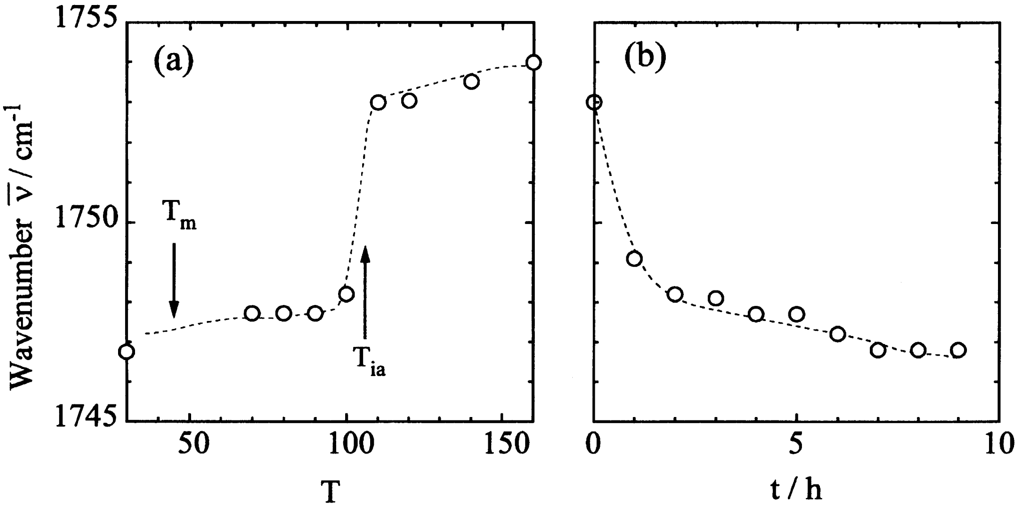

Fig. 7. The mean wavenumber $\bar{\nu}$ of the carbonyl absorption band: (a) as a function of temperature for pure CB10, and (b) as a function of time for a CB10/HD mixture ($w_1=0.42$, $T=59$ °C).

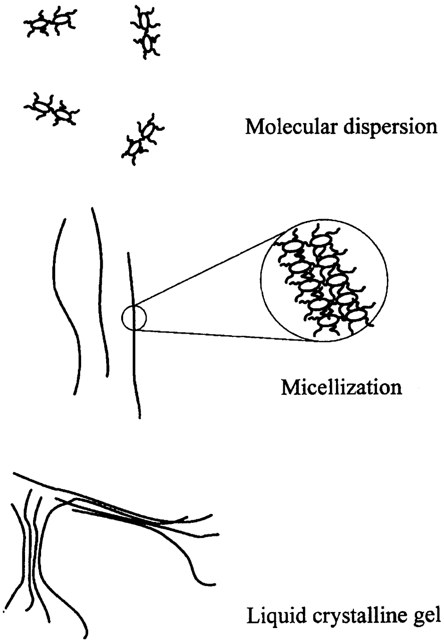

Fig. 10. Schematic representation of the micellization and gelation of the CB10/HD system.

This work was supported by a Grant-in-Aid for Scientific Research No. 05453150, from the Ministry of Education, Science and Culture.

References

1) G. A. Jeffrey, *Acc. Chem. Res.*, **19**, 168 (1986).
2) G. A. Jeffrey and L. M. Wingert, *Liq. Cryst.*, **12**, 179 (1992).
3) K. Praefcke, D. Blunk, and J. Hampel, *Mol. Cryst. Liq. Cryst.*, **243**, 323 (1994).
4) B. Kohne and K. Praefcke, *Angew. Chem.*, **96**, 70 (1984).
5) T. Itoh, A. Takada, T. Fukuda, T. Miyamoto, Y. Yakoh, and J. Watanabe, *Liq. Cryst.*, **9**, 221 (1991).
6) A. Takada, T. Itoh, T. Fukuda, T. Miyamoto, Y. Yakoh, and J. Watanabe, *Liq. Cryst.*, **12**, 337 (1992).
7) A. Takada, K. Fujii, J. Watanabe, T. Fukuda, and T. Miyamoto, *Macromolecules*, **27**, 1651 (1994).
8) V. Vill and J. Thiem, *Liq. Cryst.*, **9**, 451 (1991).
9) T. Fukuda, M. Sugiura, A. Takada, T. Itoh, Y.-D. Ma, M. Minoda, and T. Miyamoto, *Sen-i Gakkaishi*, **47**, 452 (1991).
10) A. Takada, N. Ide, J. Watanabe, T. Fukuda, and T. Miyamoto, *Liq. Cryst.*, in press.
11) H. Hasegawa, *Kobunshi*, **36**, 366 (1987).
12) T. Fukuda, Y. Tsujii, and T. Miyamoto, *Makromol. Chem.*, *Macromol. Symp.*, in press.